Preprints of the 19th World Congress
The International Federation of Automatic Control
Cape Town, South Africa. August 24-29, 2014

Robust Image-based Visual Servo Control of an Uncertain Missile Airframe

Murat T. Aygun * **William MacKunis** ** **Siddhartha Mehta** ***

* *Embry-Riddle Aeronautical University, Daytona Beach, FL 32114 USA, (e-mail: aygunm@my.erau.edu).*
** *Physical Sciences Department, Embry-Riddle Aeronautical University, Daytona Beach, FL 32114 USA, (e-mail: william.mackunis@erau.edu)*
*** *Research and Eng. Education Facility, University of Florida, Shalimar, FL 32579 USA, (e-mail: siddhart@ufl.edu)*

Abstract: A nonlinear vision-based guidance law is presented in this paper for a missile-target scenario in the presence of model uncertainty and unknown target evasive maneuvers. To this end, projective geometric relationships are utilized to combine the image kinematics with the missile dynamics in an *integrated visual dynamic system*. The guidance law is designed using an image-based visual servo control method in conjunction with a sliding-mode control strategy, which is shown to achieve asymptotic target interception in the presence of the aforementioned uncertainties. A Lyapunov-based stability analysis is presented to prove the theoretical result, and numerical simulation results are provided to demonstrate the performance of the proposed robust controller for both stationary and non-stationary targets.

Keywords: robust control, missiles, computer vision, visual servo control, image-based, guidance systems, autonomous, lyapunov stability

1. INTRODUCTION

The uncertainties and complex nonlinearities inherent in vision-based systems necessitate the development of advanced nonlinear control methods. Challenges in visual servo control design include dynamic model uncertainty, camera calibration errors, and pixel noise. Visual servo control (VSC) is the process of using vision-based feedback measurements to control a dynamic system. The information-rich nature of vision-based data has made VSC an attractive option in various industrial, medical, military, and robotic applications [Slotine et al. 1991, Yanushevsky 2007, Mackunis et al. 2007, Mebarki et al. 2010, Mehta et al. 2012b,a]. Although theoretical VSC design has been widely investigated in literature [Hutchinson et al. 1996, Chaumette and Hutchinson 2006, Chaumette et al. 2007], implementation of VSC systems was limited until recent decades due to limitations on available computational power and electronic equipment. With modern electronic capabilities, active/passive vision systems have become a more viable option [Seetharaman et al. 2006, Langelaan 2007].

Accurate representation of a missile dynamic model is a challenging task since it involves quantities that might be difficult to obtain (e.g., inertia, aerodynamic friction, external disturbances). Intelligent and adaptive control methods are popularly utilized to compensate for system uncertainty. Neural-network (NN)-based controllers exploit the universal approximation property of NNs to compensate for system uncertainty through an offline learning (training) process. Miljković et al. [2012], present a switching NN controller to support the vision-based control of a robotic manipulator using a reinforcement learning technique. They showed that the NN controller was capable of choosing the optimal course of action despite camera calibration errors, modelling errors, and image noise existing in the system. While NNs *learn* about the dynamic system through offline training, adaptive controllers can compensate for parametric uncertainty in real time using online adaptive parameter update laws. Unlike NN controllers, adaptive methods handle uncertainties without the necessity to train offline, making them a more practical control method for some applications [Zak 2003, Dixon 2007, MacKunis et al. 2010, Mehta et al. 2012a]. Mehta et al. [2012a,b] have developed an adaptive guidance law for a vision-based missile that achieves near zero miss distance interception of a target undergoing unknown evasive maneuvers.

While adaptive and NN-based control methods can compensate for system uncertainty, both methods can burden the system with a heavy computational load. Robust control methods, on the other hand, can compensate for unknown disturbances, model uncertainties and nonlinearities without the need for online adaptation or offline training.

A nonlinear vision-based guidance law is presented in this paper for a missile-target scenario in the presence of model uncertainty and unknown target evasive maneuvers. To this end, projective geometric relationships are utilized to combine the image kinematics with the missile dynamics in an *integrated visual dynamic system*. The guidance law is designed using an image-based visual servo control method in conjunction with a sliding-mode control strategy, which

is shown to achieve asymptotic target interception in the presence of the aforementioned uncertainties. A Lyapunov-based stability analysis is presented to prove the theoretical result, and numerical simulation results are provided to demonstrate the performance of the proposed robust missile guidance law for both stationary and non-stationary targets.

2. MISSILE DYNAMICS

The dynamic system being modeled consists of multiple components: The 3D space where the Euclidean motion takes place, the missile-target dynamics, and the camera system used for tracking the target. In order to relate subcomponents of the system, the following coordinate frames are defined.

An orthogonal frame $\mathcal{F}_m(t)$ is defined at the center of gravity (CoG) of the missile. An Earth-fixed reference frame $\mathcal{F}_e$ is defined on the surface of the Earth which is used to track the motion of the missile and target in 3D space.A body-fixed reference frame $\mathcal{F}_r$ is defined, located at the CoG of the missile. Frame $\mathcal{F}_r$ is fixed to a North-East-Down (NED) navigation frame, and is assumed to coincide with frame $\mathcal{F}_e$ (assuming the Earth's curvature is negligible). The body-carried reference frame $\mathcal{F}_r$ is used to define the angular orientation of the aircraft, while the Earth-fixed reference frame $\mathcal{F}_e$ is used to define its translation. For model simplification and without loss of generality, the camera frame $\mathcal{F}_c(t)$ is defined at the center of gravity of the missile, coinciding with the frames $\mathcal{F}_m(t)$ and $\mathcal{F}_r$.

The dynamic model for a bank-to-turn missile (BTT) is used. The orientation of frame $\mathcal{F}_m$ with respect to frame $\mathcal{F}_r$ is defined by angles of rotation $\phi(t)$, $\sigma(t)$, and $\psi(t)$ about the body-fixed x, y, and z-axes, respectively.

The linear and angular velocities of the missile measured in $\mathcal{F}_m$ with respect to $\mathcal{F}_e$ are denoted by

$$v_m = [v_x \quad v_y \quad v_z]^T \in \mathbb{R}^3 \quad \omega_m = [\omega_x \quad \omega_y \quad \omega_z]^T \in \mathbb{R}^3 \tag{1}$$

The linear acceleration of the missile measure in the body frame $\mathcal{F}_m(t)$ is expressed as

$$\begin{aligned} \dot{v}_x &= \omega_z v_y - \omega_y v_z + \frac{F_x}{m} \\ \dot{v}_y &= \omega_x v_z - \omega_z v_x + \frac{F_y}{m} \\ \dot{v}_z &= \omega_y v_x - \omega_x v_y + \frac{F_z}{m} \end{aligned} \tag{2}$$

In the equations above, $m \in \mathbb{R}$ represents the constant mass of the missile, and $F_x(t)$, $F_y(t)$, $F_z(t) \in \mathbb{R}$ are the forces acting along the body axes defined as

$$\begin{aligned} F_x &= G_x(q) + k_F \rho_{air} V_M^2 C_x(\alpha, \beta, M_m) + \tau_x \\ F_y &= G_y(q) + k_F \rho_{air} V_M^2 C_y(\alpha, \beta, M_m) + \tau_y \\ F_z &= G_z(q) + k_F \rho_{air} V_M^2 C_z(\alpha, \beta, M_m) + \tau_z \end{aligned} \tag{3}$$

where $k_F \in \mathbb{R}$ is a constant parameter determined by the missile geometry, $\rho_{air} \in \mathbb{R}$ is the air density, and $V_M(t) \in \mathbb{R}$ is the magnitude of the missile velocity measured with respect to $\mathcal{F}_e$. $C_x(\alpha, \beta, M_m)$, $C_y(\alpha, \beta, M_m)$, $C_z(\alpha, \beta, M_m) \in \mathbb{R}$ are the unknown friction coefficients corresponding to the aerodynamic forces, where $\alpha(t)$, $\beta(t)$, and $M_m(t)$ represent the angle of attack, sideslip angle, and Mach number, respectively. $\tau_x(t)$, $\tau_y(t)$, $\tau_z(t) \in \mathbb{R}$ are the control force inputs. The x, y, and z components of the gravitational force acting on the missile, $G_x(t)$, $G_y(t)$, $G_z(t) \in \mathbb{R}$ are expressed as

$$\begin{aligned} G_x(t) &= -mg\sin(\sigma) \\ G_y(t) &= -mg\cos(\sigma)\sin(\phi) \\ G_z(t) &= -mg\cos(\sigma)\cos(\phi) \end{aligned} \tag{4}$$

where $g \in \mathbb{R}$ is the gravitational acceleration constant.

The angular acceleration of the missile measured in $\mathcal{F}_m$ with respect to $\mathcal{F}_e$ is denoted by

$$\begin{aligned} \dot{\omega}_x &= \frac{I_y - I_z}{I_x}\omega_y\omega_z + \frac{L}{I_x} \\ \dot{\omega}_y &= \frac{I_z - I_x}{I_y}\omega_x\omega_z + \frac{M}{I_y} \\ \dot{\omega}_z &= \frac{I_x - I_y}{I_z}\omega_x\omega_y + \frac{N}{I_z} \end{aligned} \tag{5}$$

where I_x, I_y, $I_z \in \mathbb{R}$ denote the constant unknown moments of inertia about the x, y, and z-axes, respectively. $L(t)$, $M(t)$, $N(t) \in \mathbb{R}$ are the rolling, pitching and yawing moments, respectively, given by

$$\begin{aligned} L &= k_M \rho_{air} V_M^2 C_l(\alpha, \beta, M_m) + \tau_l \\ M &= k_M \rho_{air} V_M^2 C_m(\alpha, \beta, M_m) + \tau_m \\ N &= k_M \rho_{air} V_M^2 C_n(\alpha, \beta, M_m) + \tau_n. \end{aligned} \tag{6}$$

In (6), $C_l(\alpha, \beta, M_m)$, $C_m(\alpha, \beta, M_m)$, $C_n(\alpha, \beta, M_m) \in \mathbb{R}$ denote unknown coefficients of friction corresponding to the aerodynamic moments; and $\tau_l(t)$, $\tau_m(t)$, $\tau_n(t) \in \mathbb{R}$ are the control moment inputs.

The equation of motion for the missile can now be expressed in Euler-Lagrange form, considering the coordinate frames and dynamical equations defined above, as

$$M\ddot{q} = C(\dot{q})\dot{q} + G(q) + f(\dot{q}) + \tau + \tau_d \tag{7}$$

where $q(t)$, $\dot{q}(t) \in \mathbb{R}^6$ denote the 6-DOF position and velocity, respectively, of frame $\mathcal{F}_m(t)$ with respect to frame $\mathcal{F}_e$ and $\tau \in \mathbb{R}^6$ represents the vector of control force inputs [1] where

$$\begin{aligned} q(t) &= [x \quad y \quad z \quad \phi \quad \sigma \quad \psi]^T \\ \dot{q}(t) &= [v_m^T \quad \omega_m^T]^T \\ \tau(t) &= [\tau_x \quad \tau_y \quad \tau_z \quad \tau_l \quad \tau_m \quad \tau_n]^T \end{aligned} \tag{8}$$

In (7), $\tau_d(t) \in \mathbb{R}^6$ denotes an unknown, nonlinear, nonvanishing bounded disturbance (e.g., due to unknown evasive target maneuvers). Also in (7), $M \in \mathbb{R}^{6x6}$ represents the unknown constant inertia matrix, $C(\dot{q}) \in \mathbb{R}^{6x6}$ is the Coriolis matrix, $G(q) \in \mathbb{R}^6$ is the unknown gravity vector, and $f(\dot{q}) \in \mathbb{R}^6$ denotes the unknown friction vector, which are defined as

$$M = diag(m, m, m, I_x, I_y, I_z) \tag{9}$$

$$C(\dot{q}) = diag(-[m\omega_m]_\times, [mv_m]_\times) \tag{10}$$

[1] It should be noted that the control force input, τ, is assumed to be decoupled in this preliminary study (i.e., the control can be applied in 6-DoF independently). The 6-DoF independent control is commonly used in order to simplify the dynamic model (Mehta et al. [2011], Mehta et al. [2012a], Mehta et al. [2012b]). However, use of a realistic dynamic model is intended for future studies in which deflection surface angles are used to steer the missile [Yanushevsky 2007]).

$$G(q) = \begin{bmatrix} -mg\sin(\sigma) \\ mg\cos(\sigma)\sin(\phi) \\ mg\cos(\sigma)\cos(\phi) \\ 0 \\ 0 \\ 0 \end{bmatrix} \quad f(\dot{q}) = \begin{bmatrix} k_F\rho_{air}v_x^2C_x \\ k_F\rho_{air}v_x^2C_y \\ k_F\rho_{air}v_x^2C_z \\ k_F\rho_{air}v_x^2C_l \\ k_F\rho_{air}v_x^2C_m \\ k_F\rho_{air}v_x^2C_n \end{bmatrix} \tag{11}$$

In (9) and (10), $diag(\cdot)$ represents a diagonal matrix, and $[\cdot]_\times$ denotes the skew-symmetric cross-product matrix.

3. IMAGE KINEMATICS

This section formulates the relationships between the missile velocity $\dot{q}(t) \in \mathbb{R}^6$ and the velocity of the target $\mathcal{T}$ in the camera image plane. A monocular camera is attached to the center of gravity of the missile airframe [2].

A time-varying orthogonal frame $\mathcal{F}_c(t)$ is attached to the camera such that the origins of $\mathcal{F}_c(t)$ and the missile body frame $\mathcal{F}_m(t)$ coincide with the missile center of gravity. A target $\mathcal{T}$ is represented as a point in Euclidean space, and it is assumed to remain within the camera field of view. [3]

The Euclidean coordinates of the target $\mathcal{T}$ expressed in the camera coordinate frame $\mathcal{F}_c(t)$ can be represented as

$$\bar{m}(t) \triangleq [x_t(t) \quad y_t(t) \quad z_t(t)]^T \tag{12}$$

where it is assumed that the target is always in front of the camera (i.e., $z_t(t) > \epsilon$, $\epsilon \in \mathbb{R}^+$). The rate of change of the Euclidean coordinates $\bar{m}(t)$ due to the camera motion is related to the camera velocity as [Mehta et al. 2012a]

$$\dot{\bar{m}}(t) = -v_c(t) - \omega_c(t) \times \bar{m}(t) \tag{13}$$

where $v_c(t)$, $\omega_c(t) \in \mathbb{R}^3$ are linear and angular velocities, respectively, of the camera as measured in $\mathcal{F}_c(t)$. By using a transformation of a left-hand coordinate frame to a right-hand coordinate frame, the camera coordinate frame can be related to the 6-DOF missile velocity as measured in $\mathcal{F}_m(t)$ as

$$v_c = [v_y \quad -v_z \quad v_x]^T \quad and \quad \omega = [\omega_y \quad -\omega_z \quad \omega_x]^T \tag{14}$$

The target $\mathcal{T}$ is projected onto an image plane π as the point

$$p(t) \triangleq [u(t) \quad v(t)]^T \tag{15}$$

where pixel coordinates $p(t)$ are related to the Euclidean coordinates $\bar{m}(t)$ by projection geometry as

$$u(t) = \frac{f_o a x_t(t)}{z_t(t)} + u_0 \quad v(t) = \frac{f_o b y_t(t)}{z_t(t)} + v_0 \tag{16}$$

where $f_o \in \mathbb{R}$ is the focal length, a and $b \in \mathbb{R}$ are scaling factors along x and y-axes; and $[u_0, v_0]^T \in \mathbb{R}^2$ are the principal point coordinates (i.e., the intersection of an optical axis with the image plane) of the camera. After taking the time derivative of $p(t)$, the following expression for the rate of change of the pixel coordinates is obtained:

$$\dot{p}(t) = \begin{bmatrix} \dot{u}(t) \\ \dot{v}(t) \end{bmatrix} = J\dot{q}(t) \tag{17}$$

[2] Although the camera is typically placed at the nose of the missile in practical implementation, this assumption can be made without the loss of generality, since any deviation can be accounted for by a simple coordinate transformation.

[3] This is to ensure the closed-loop behavior of the system. Some existing vision-based controllers have a potential field implemented around the FOV within the control law to ensure feature points stay in the image plane (Corke and Hutchinson [2001]).

where $J \in \mathbb{R}^{2\times 6}$ denotes the Jacobian matrix which contains the projection geometry defined using (16) as

$$J = \begin{bmatrix} \frac{f_o a x_t}{z_t^2} & -\frac{f_o a}{z_t} & 0 & \frac{f_o a y_t}{z_t} & \frac{f_o a x_t y_t}{z_t^2} & a(f_o + \frac{f_o x_t^2}{z_t^2}) \\ \frac{f_o b y_t}{z_t^2} & 0 & \frac{f_o b}{z_t} & -\frac{f_o b x_t}{z_t} & b(f_o + \frac{f_o y_t^2}{z_t^2}) & \frac{f_o b x_t y_t}{z_t^2} \end{bmatrix} \tag{18}$$

It is assumed that the image Jacobian $J(u, v, z_t)$ is measurable. The estimation of depth is a challenging task using a monocular camera. Any uncertainties due to inaccurate depth information are assumed to be absorbed into the unknown auxiliary terms $\tilde{N}$ and N_d, which are introduced in the control development section. These terms are compensated by the robust control law design. Future work will consider using a homography-based approach, which utilizes minimal feature point information about the target in order to calculate depth information [Mackunis et al. 2007].

The image Jacobian J given above remains bounded everywhere except at $z_t = 0$. [4] This occurs when the camera frame $\mathcal{F}_c(t)$ intercepts the target $\mathcal{T}$. However, the impact actually happens before $\mathcal{F}_c(t)$ intercepts the target, since the origin of $\mathcal{F}_c(t)$ is at the missile CoG. Therefore, the missile is considered to have intercepted the target when $0 < z_t \leq z_{min}$, $z_{min} \in \mathbb{R}^+$.

4. CONTROL OBJECTIVE

The control objective of this system is to drive the relative distance between the missile frame $\mathcal{F}_m$ and the target frame $\mathcal{T}$ to zero. This can be achieved by driving the time-varying target pixel coordinates $p(t)$ to the desired image coordinates p_d, which is constant(i.e., the optical axis). Therefore, the control objective can be mathematically stated as:

$$p(t) \longrightarrow p_d, \quad where \quad p_d = [u_0 \quad v_0]^T. \tag{19}$$

5. CONTROL DEVELOPMENT

Property 1: The inertia matrix M is symmetric, positive definite, such that for known positive constants m_1, $m_2 \in \mathbb{R}$, the following inequality satisfied:

$$m_1\|\xi^2\| \leq \xi^T M \xi \leq m_2\|\xi^2\| \quad \forall \xi \in \mathbb{R}^n \tag{20}$$

To quantify the control objective, a tracking error term $e(t) \triangleq [e_1 \quad e_2]^T \in \mathbb{R}^2$ is defined as the difference between the image coordinates of the target and the principal point as

$$e(t) \triangleq p_d - p(t). \tag{21}$$

After taking the time derivative of (21) and using the image kinematic equation in (17), we obtain

$$\dot{e}(t) = -\dot{p}(t) = -J\dot{q}. \tag{22}$$

To facilitate the subsequent control development and stability analysis, we add and subtract λe in (22) to yield

$$\dot{e}(t) = -J\dot{q} + \lambda e - \lambda e \tag{23}$$

where $\lambda \in \mathbb{R}$ is a positive constant control gain. An auxiliary error term $r(t) \in \mathbb{R}^6$ is introduced to facilitate

[4] In light of this, pseudo-inverse of $J(t)$ is singularity free.

the following controller development and stability analysis as

$$r(t) = -\dot{q} + J^{+}\lambda e \tag{24}$$

where $J^{+}(t) \in \mathbb{R}^{6\times 2}$ denotes the pseudo-inverse of the Jacobian matrix $J(t)$. By using (23) and (24), the rate of change of error term $e(t)$ can be expressed as

$$\dot{e}(t) = -\lambda e + Jr. \tag{25}$$

By pre-multiplying the auxiliary error signal $r(t)$ by M and taking the time derivative, the open-loop error dynamics are obtained as

$$M\dot{r} = -M\ddot{q} + M\dot{J}^{+}\lambda e + MJ^{+}\lambda\dot{e} \tag{26}$$

By substituting (7) into (26) the open-loop error dynamics can be expressed as

$$M\dot{r} = -J^{T}e - \tau + \tilde{N} + N_d \tag{27}$$

where the unknown, unmeasurable auxiliary terms $\tilde{N}(t)$, $N_d(t) \in \mathbb{R}^6$ are defined as

$$\begin{aligned}\tilde{N} = & -C\dot{q} + C\dot{q}_d - G(q) + G(q_d) - f(\dot{q}) + f(\dot{q}_d) \\ & + M\dot{J}^{+}\lambda e - M\dot{J}^{+}(q_d)\lambda e + MJ^{+}\lambda\dot{e} - MJ^{+}\lambda\dot{e}(q_d) \\ & + J^{T}e - J^{T}(q_d)e\end{aligned} \tag{28}$$

and

$$\begin{aligned}N_d = & -C\dot{q}_d - G(q_d) - f(\dot{q}_d) + \tau_d \\ & + M\dot{J}^{+}(q_d)\lambda e + MJ^{+}\lambda\dot{e}(q_d) + J^{T}(q_d)e\end{aligned} \tag{29}$$

The terms q_d and $\dot{q}_d$ represent desired 6-DoF position and velocity vectors respectively which are assumed to be bounded and sufficiently smooth. The selective grouping of the terms in (28) and (29) is motivated by the fact that the following inequalities can be developed [MacKunis et al. 2010]

$$\|\tilde{N}\| \leq \rho(\|z\|)\|z\|, \quad \|N_d\| \leq \zeta_d \tag{30}$$

where $\rho(\cdot) \in \mathbb{R}$ is a bounding function, and $\zeta_d \in \mathbb{R}$ is a known positive bounding constant. In (30), $z(t) \in \mathbb{R}^8$ denotes an augmented error vector defined as

$$z(t) \triangleq [e^{T} \quad r^{T}]^{T}. \tag{31}$$

Based on the open-loop error system in (27) and the subsequent stability analysis, the control input $\tau(t) \in \mathbb{R}^6$ is designed as

$$\tau = (k_s + 1)r + \beta_s sgn(r) \tag{32}$$

where k_s, $\beta_s \in \mathbb{R}$ are positive constant control gains; and $sgn(\cdot)$ denotes the vector form of the standard signum function, where the $sgn(\cdot)$ is applied to each element of the vector argument. The use of $sgn(\cdot)$ fucntion is motivated by the desire to compensate the unknown bounded target maneuvers without the use of adaptive laws or function approximators. After substituting the control law in (32) into the open-loop error dynamics in (27), the closed-loop error system is obtained as

$$M\dot{r} = \tilde{N} + N_d - J^{T}e - (k_s + 1)r - \beta_s sgn(r). \tag{33}$$

To facilitate the following stability analysis, the control gain β_s is selected to satisfy

$$\beta_s > \zeta_d \tag{34}$$

where ζ_d is introduced in (30).

6. STABILITY ANALYSIS

Theorem 1. The controller presented in (32) ensures that the missile airframe F_m asymptotically intercepts the target in the sense that

$$\lim_{t\to\infty} r(t), e(t) = 0 \tag{35}$$

Proof 1. Consider a non-negative function $V(t)$ (i.e., Lyapunov function) defined as

$$V(t) = \frac{1}{2}r^{T}Mr + \frac{1}{2}e^{T}e. \tag{36}$$

After taking the time derivative of $V(t)$, using (25) and (33) and cancelling common terms, $\dot{V}(t)$ can be expressed as

$$\dot{V} = r^{T}\tilde{N} + r^{T}N_d - r^{T}(k_s+1)r - r^{T}\beta_s sgn(r) - e^{T}\lambda e. \tag{37}$$

By using the inequalities defined in (30), $\dot{V}(t)$ can be upper bounded as

$$\dot{V} \leq -\lambda_0\|z\|^2 + \frac{\rho^2(\|z\|)}{4k_s}\|z\|^2 \tag{38}$$

where $\lambda_0 \triangleq min\{1, \lambda\}$. Based on Inequality (38), the control gain k_s can be selected to render $\dot{V}(t) < 0$. Specifically, by designing k_s to satisfy

$$k_s > \frac{\rho^2(\|z\|)}{4\lambda_0} \tag{39}$$

the upper bound on $\dot{V}(t)$ can be expressed as

$$\dot{V} \leq -C\|z\|^2 \tag{40}$$

where $C \in \mathbb{R}$ is a positive bounding constant. Thus, provided k_s satisfies (39), $\dot{V}(t)$ is negative definite. Hence, $\|z(t)\| \to 0$ as $t \to \infty$, and $\|r(t)\|$, $\|e(t)\| \to 0$ as $t \to \infty$ from (31).

The expressions in (36) and (40) can be used to prove that $e(t)$, $r(t) \in \mathcal{L}_\infty$ during closed-loop controller operation. Given that $e(t)$, $r(t) \in \mathcal{L}_\infty$, (22) and (25) can be used to conclude that $\dot{e}(t)$, $\dot{p}(t) \in \mathcal{L}_\infty$. Standard linear analysis techniques can then be used to show that $\dot{q}(t) \in \mathcal{L}_\infty$ from (22). Given that $r(t) \in \mathcal{L}_\infty$, $\tau(t) \in \mathcal{L}_\infty$ from (32).

7. SIMULATION - STATIONARY TARGET

The performance of the proposed robust control law was tested via numerical computer simulation using Matlab. The first simulation involved a stationary target located at a Euclidean point with respect to the NED Earth frame given by

$$[x_t \quad y_t \quad z_t]^{T} = [1200 \quad 2400 \quad -5000]^{T}(m) \tag{41}$$

The missile body frame $\mathcal{F}_m(t)$ is initialized at the position

$$[x_m(0) \quad y_m(0) \quad z_m(0)]^{T} = [0 \quad 0 \quad -3500]^{T}(m) \tag{42}$$

and the initial missile orientation is

$$R_m = \begin{bmatrix} 0.5000 & -0.8138 & 0.2942 \\ 0.8660 & 0.4698 & -0.1710 \\ 0 & 0.3420 & 0.9397 \end{bmatrix}. \tag{43}$$

The modeling parameters used in the simulation environment are given by

$$\begin{array}{llll} m = 144.0 & [kg] & g = 9.81 & [m/s^2] \\ I_x = 1.615 & [kg-m^2] & \rho_{air} = 0.26 & [kg/m^3] \\ I_y = 136.0 & [kg-m^2] & k_F = 0.01425 & [m^2] \\ I_z = 136.0 & [kg-m^2] & k_M = 2.716\times 10^{-3} & [m^3] \\ k_s = 30 & [\cdot] & \beta_s = 600 & [\cdot] \end{array} \tag{44}$$

where m is mass of the missile, g is the gravitational acceleration, I_x, I_y, and I_z are the missile moment of inertia about the x, y, and z-axes, respectively. The density of air is represented by ρ_{air}, while k_F and k_M are constant

missile parameters. The aerodynamic friction coefficients are obtained using

$$\begin{aligned} C_x &= -0.57 + 0.0083\alpha \\ C_y &= -0.21\beta \\ C_z &= (0.0429 - 0.5052\alpha + 0.0125\alpha^2 - 0.0015\alpha^3) \\ &\quad +(-0.0191 - 0.1230\alpha - 0.0138\alpha^2 + 0.0006\alpha^3)M_m \\ C_l &= 0.116\beta \\ C_m &= (-0.0381 - 2.7419\alpha + 0.2131\alpha^2 - 0.0055\alpha^3) \\ &\quad +(-0.4041 + 0.8715\alpha - 0.0623\alpha^2 + 0.0014\alpha^3)M_m \\ C_n &= 0.08\beta \end{aligned} \tag{45}$$

The coefficients of friction in (45) and the missile dynamic parameters are used only to generate the plant model; they are not used in the guidance law. The simulation includes additive white Gaussian noise (AWGN) in the target pixel coordinate $p(u, v)$ with a standard deviation of 0.1 pixel and AWGN in the depth measurement $z(t)$ with a standard deviation of 10m. Simulation results show that robust control law compensates for unmodeled effects and the AWGN added into the system.

Figure 1 shows the initial target position ($\square$) and the final position of the target ($\triangle$) in the image plane. It is observed that the controller is able to drive the target image to the desired image location at the principal point u_0, v_o. The control input required to track the target is plotted in Figure 2. The proposed robust control

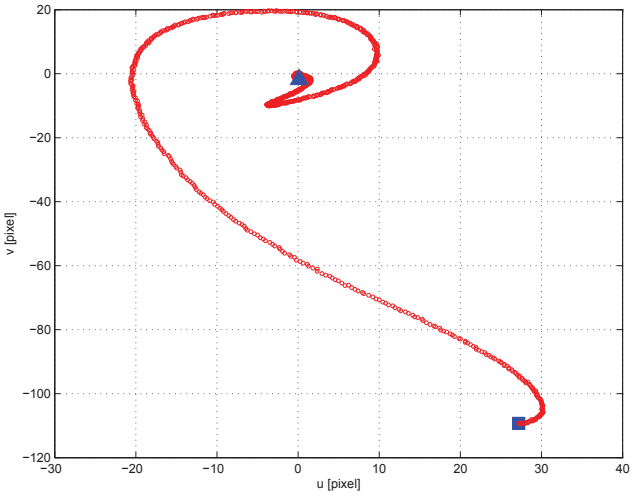

Fig. 1. Tracking of the stationary target in the image plane.

system is shown to be capable of tracking the target and achieving interception in the presence of the uncertainties and modeling errors introduced into the simulated system. In this section, the simulation considered the case where the target is stationary. The next section considers a non-stationary target.

8. SIMULATION - NON-STATIONARY TARGET

The second simulation involved the evaluation of the proposed controller's performance in the presence of a moving target. The simulation parameters are identical to the first one with the addition of a moving target. The target translational and angular velocities, v_t and ω_t, used in the simulation are given as

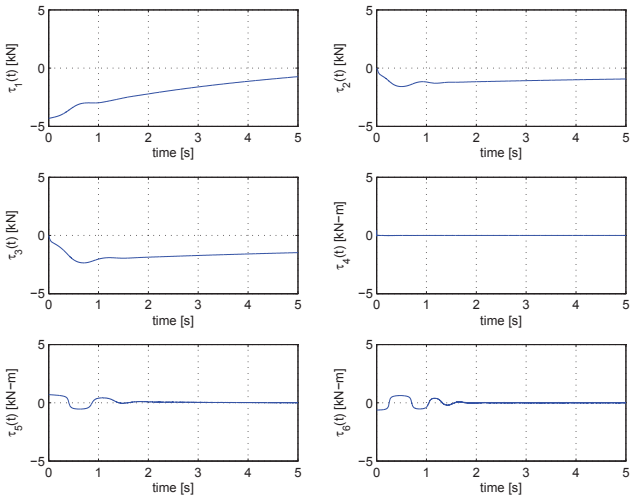

Fig. 2. The control input commands during closed-loop operation.

$$v_t = [50 \quad 30 \quad 0]^T(m/s), \quad \omega_t = [0 \quad 0 \quad 0.05]^T(rad/s) \tag{46}$$

The target velocity is used to generate the simulation plant model only; the target velocities are assumed unknown and are not used in the control law.

Figure 3 shows the tracking performance of the proposed controller in the presence of a moving target. It can be seen that the controller drives the target toward the principal point, and that the error is reduced asymptotically. Thus, the missile intercepts the target with zero miss distance. The trajectory of the missile in Euclidean space is plotted in Figure 5. It was shown that the missile frame is able to track the moving target and intercept it. The control commands used during closed-loop operation are plotted in Figure 4.

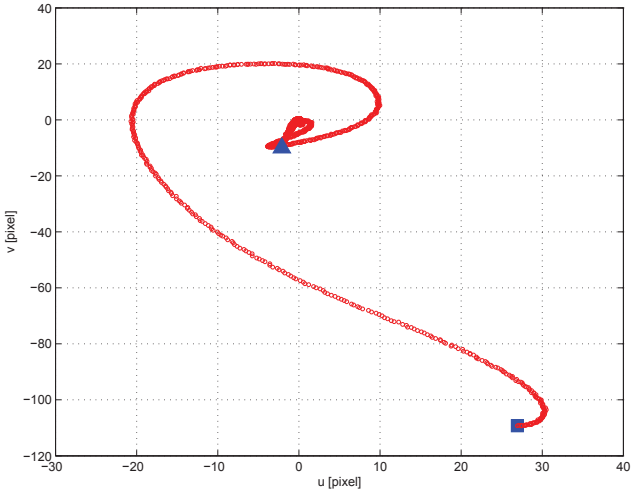

Fig. 3. Tracking of the non-stationary target in the image plane.

9. CONCLUSION

A robust vision-based missile guidance law is presented for a missile equipped with a monocular camera system. The guidance law yields asymptotic target interception

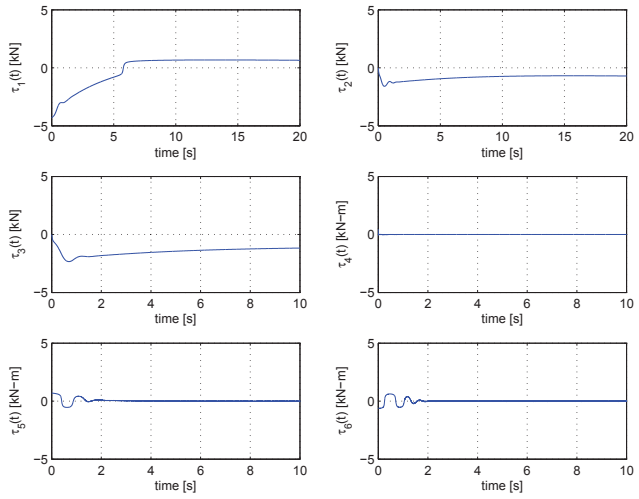

Fig. 4. The control commands used during closed-loop controller operation.

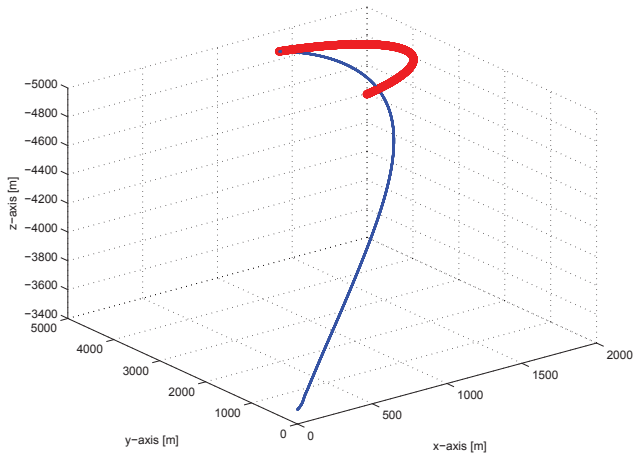

Fig. 5. 3D visualisation of the missile trajectory (*in blue*) and interception of the non-stationary target (*in red*).

of a target in the presence of dynamic uncertainty and unknown target evasive maneuvers. The result is achieved by using an image-based visual servo control method, where the missile dynamics are combined with the target image kinematics of the monocular camera. The proposed control law is designed to be inexpensively implemented, requiring no online adaptive laws, NNs, or complex computations in the control loop. A Lyapunov-based stability analysis is used to prove that the proposed control law is capable of regulating the pixel coordinates of the target to the principle point. Once the target image coordinates are driven toward the principal point (optical axis), then the missile converges to a collision course. A numerical simulation is used to test the performance of the control law in the presence of stationary and non-stationary targets, where the plant model contains modeling errors and additive disturbances. The simulation results demonstrate that the proposed vision-based robust pursuit guidance law is capable of intercepting the target in both cases with zero miss distance.

REFERENCES

Chaumette, F. and Hutchinson, S. (2006). Visual servo control. i. basic approaches. *Robotics & Automation Magazine, IEEE*, 13(4), 82–90.

Chaumette, F., Hutchinson, S., et al. (2007). Visual servo control, part ii: Advanced approaches. *IEEE Robotics and Automation Magazine*, 14(1), 109–118.

Corke, P.I. and Hutchinson, S.A. (2001). A new partitioned approach to image-based visual servo control. *Robotics and Automation, IEEE Transactions on*, 17(4), 507–515.

Dixon, W.E. (2007). Adaptive regulation of amplitude limited robot manipulators with uncertain kinematics and dynamics. *Automatic Control, IEEE Transactions on*, 52(3), 488–493.

Hutchinson, S., Hager, G.D., and Corke, P.I. (1996). A tutorial on visual servo control. *Robotics and Automation, IEEE Transactions on*, 12(5), 651–670.

Langelaan, J.W. (2007). State estimation for autonomous flight in cluttered environments. *Journal of guidance, control, and dynamics*, 30(5), 1414–1426.

Mackunis, W., Gans, N., Kaiser, K., and Dixon, W. (2007). Unified tracking and regulation visual servo control for wheeled mobile robots. In *Control Applications, 2007. CCA 2007. IEEE International Conference on*, 88–93. IEEE.

MacKunis, W., Wilcox, Z., Kaiser, M., and Dixon, W. (2010). Global adaptive output feedback tracking control of an unmanned aerial vehicle. *Control Systems Technology, IEEE Transactions on*, 18(6), 1390–1397.

Mebarki, R., Krupa, A., and Chaumette, F. (2010). 2-d ultrasound probe complete guidance by visual servoing using image moments. *Robotics, IEEE Transactions on*, 26(2), 296–306.

Mehta, S., MacKunis, W., Pasiliao, E., and Curtis, J. (2012a). Adaptive image-based visual servo control of an uncertain missile airframe. In *Guidance, Navigation and Control Conf.(GNC), Proc. of AIAA, Minneapolis, MN*.

Mehta, S., MacKunis, W., Subramanian, S., and Pasiliao, C. (2012b). Nonlinear control of hypersonic missiles for maximum target penetration. In *Guidance, Navigation and Control Conf.(GNC), Proc. of AIAA, Minneapolis, MN*.

Mehta, S., MacKunis, W., and Curtis, J. (2011). Adaptive vision-based missile guidance in the presence of evasive target maneuvers. In *World Congress, Proc. of 18th IFAC, Milano, Italy*, 5471–5476.

Miljković, Z., Mitić, M., Lazarević, M., and Babić, B. (2012). Neural network reinforcement learning for visual control of robot manipulators. *Expert Systems with Applications*.

Seetharaman, G., Lakhotia, A., and Blasch, E.P. (2006). Unmanned vehicles come of age: The darpa grand challenge. *Computer*, 39(12), 26–29.

Slotine, J.J.E., Li, W., et al. (1991). *Applied nonlinear control*, volume 199. Prentice hall New Jersey.

Yanushevsky, R. (2007). *Modern missile guidance*. CRC Press.

Zak, S.H. (2003). *Systems and control*, volume 388. Oxford University Press New York.